Experiment 4B: The rotational-vibrational spectrum of HCl

Sam White (Author) and Emma Winful (Laboratory Partner)

30/11/2018

Abstract

The rotational constants, $\tilde{B}_\nu$, were determined for both common isotopologues of HCl gas and hence the bond force constants, k. The rotational constants for $H^{35}Cl$ were in agreement with published values and the bond force constants found were $477.383 \pm 0.001 \, \mathrm{N\,m^{-1}}$ and $480.698 \pm 0.006 \, \mathrm{N\,m^{-1}}$ for $H^{35}Cl$ and $H^{37}Cl$ respectively. The bond force constants are not identical within reasonable errors, hence it is likely that the isotopic mass effects the value of k, however additional data should be collected to verify this.

1 Results and Analysis

1.1 Collected Data

Table 1: Rotational-vibrational absorbance wavelengths for the fundamental transition bands.

	J	$R(J)$ / cm^{-1}	$P(J)$ / cm^{-1}	$R(J) - P(J)$ / cm^{-1}	$R(J-1) - P(J+1)$ / cm^{-1}
$H^{35}Cl$	0	2906.4			
	1	2926.03	2865.24	60.79	62.64
	2	2945.05	2843.76	101.29	104.33
	3	2963.42	2821.70	141.72	145.98
	4	2981.14	2799.07	182.07	187.53
	5	2998.19	2775.89	222.30	228.97
	6	3014.57	2752.17	262.40	270.26
	7	3030.27	2727.93	302.34	311.4
	8	3045.28	2703.17	342.11	352.37
	9	3059.52	2677.90	381.62	393.13
	10	3073.10	2652.15	420.95	433.62
	11	3085.88	2625.90	459.98	473.88
	12		2599.22		
$H^{37}Cl$	0	2904.29			
	1	2923.91	2863.20	60.71	62.53
	2	2942.90	2841.76	101.14	104.19
	3	2961.24	2819.72	141.52	145.76
	4	2978.93	2797.14	181.79	187.25
	5	2995.96	2773.99	221.97	228.62
	6	3012.32	2750.31	262.01	269.86
	7	3027.98	2726.10	301.88	310.95
	8	3042.97	2701.37	341.60	351.84
	9	3057.22	2676.14	381.08	392.57
	10	3070.73	2650.40	420.33	432.99
	11	3083.51	2624.23	459.28	473.20
	12		2597.53		

Table 2: Rotational-vibrational absorbance wavelengths for the overtone transition bands.

	J	$R(J)$ / cm^{-1}	$P(J)$ / cm^{-1}	$R(J) - P(J)$ / cm^{-1}	$R(J-1) - P(J+1)$ / cm^{-1}
H^{35}Cl	0	5688.16			
	1	5706.59	5647.71	58.88	62.66
	2	5723.78	5625.50	98.28	104.35
	3	5739.75	5602.24	137.51	145.98
	4	5754.53	5577.80	176.73	187.53
	5	5767.89	5552.22	215.67	229.05
	6	5780.07	5525.48	254.59	270.26
	7	5790.92	5497.63	293.29	311.52
	8		5468.55		
H^{37}Cl	0	5684.12			
	1	5703.13	5643.60	59.53	62.58
	2	5719.67	5621.54	98.13	104.80
	3	5735.61	5598.33	137.28	145.76
	4	5750.30	5573.91	176.39	197.19
	5	5763.27	5548.42	214.85	228.64
	6	5775.12	5521.66	253.46	269.43
	7	5786.65	5493.84	292.81	310.49
	8		5464.63		

1.2 Determination of Rotational Constants and Bond Lengths

The values of the rotational constants $\tilde{B}_0$, $\tilde{B}_1$ and $\tilde{B}_2$ were calculated accounting for the centrifugal distortion of the molecules by plotting graphs of $\frac{R(J)-P(J)}{J+\frac{1}{2}}$ and $\frac{R(J-1)-P(J+1)}{J+\frac{1}{2}}$ against $(J+\frac{1}{2})^2$ and performing linear regressions (as shown in figures 1 and 2). This was completed since if combination differences between the $R(J)$ and $P(J)$ and then the $R(J-1)$ and $P(J+1)$ bands are taken and the centrifugal distortion accounted for the resultant equations can be re-arranged to give equations 1.2.1 and 1.2.2 respectively, where $\tilde{D}_\nu$ are the centrifugal distortion coefficients. These equations are in the form of the general equation of a straight line, $y = mx + c$, hence the plotted data can be fitted by a function of this form.

$$\frac{R(J) - P(J)}{J + \frac{1}{2}} = -8\tilde{D}_1(J + \frac{1}{2})^2 + 4\tilde{B}_1 - 6\tilde{D}_1 \tag{1.2.1}$$

$$\frac{R(J-1) - P(J+1)}{J + \frac{1}{2}} = -8\tilde{D}_0(J + \frac{1}{2})^2 + 4\tilde{B}_0 - 6\tilde{D}_0 \tag{1.2.2}$$

The values of $\tilde{D}_\nu$ were then determined (see table 6 in the supplementary information) and hence the rotational constants, $\tilde{B}_\nu$, shown in table 3 were calculated. The error propagation shown in equation 1.2.3 was then completed to estimate the uncertainties in $\tilde{B}_\nu$, where $\alpha_{\tilde{B}_\nu}$, α_m and α_c are the uncertainties in $\tilde{B}_\nu$, the gradient of the fitted line and the intercept respectively.

$$\alpha_{\tilde{B}_\nu} = \sqrt{\left(\frac{3}{16}\alpha_m\right)^2 + \left(\frac{1}{4}\alpha_c\right)^2} \tag{1.2.3}$$

The literature values of $\tilde{B}_\nu$ for H^{35}Cl in table 3 were determined using published equilibrium rotational constant, $\tilde{B}_e$, and rotational constant parameter, α_e, values[1] with equation 1.2.4.

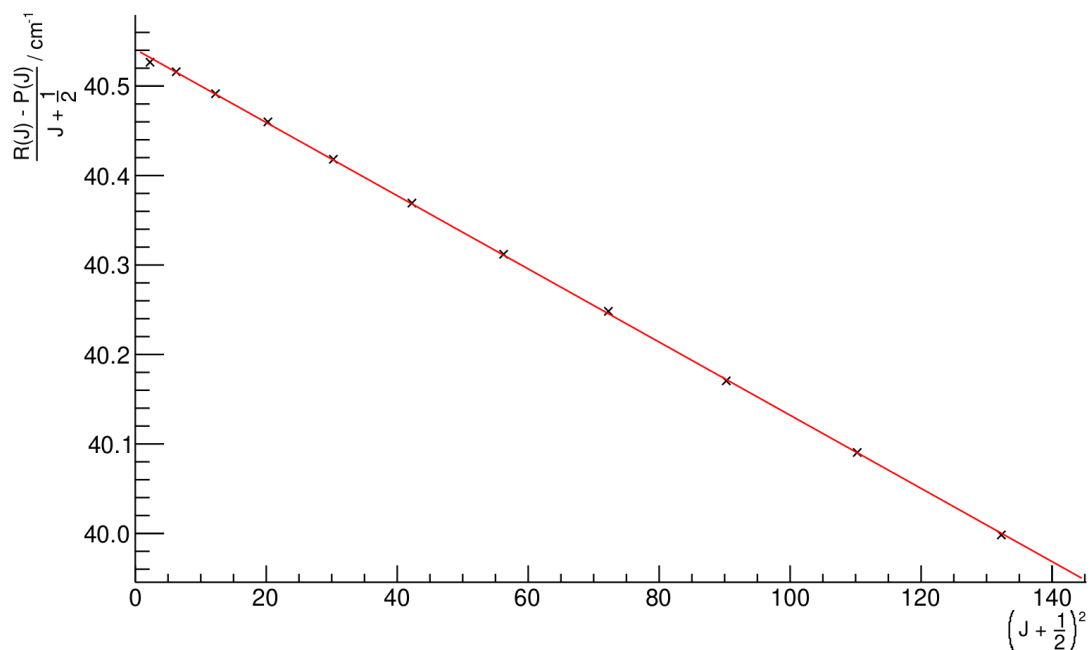$$\tilde{B}_{\nu_{Lit.}} = \tilde{B}_e - \alpha_e\left(\nu + \frac{1}{2}\right) \tag{1.2.4}$$

Figure 1: Graph showing the linear regression performed for the upper rotational (R) branch of the fundamental transition in $H^{35}Cl$.
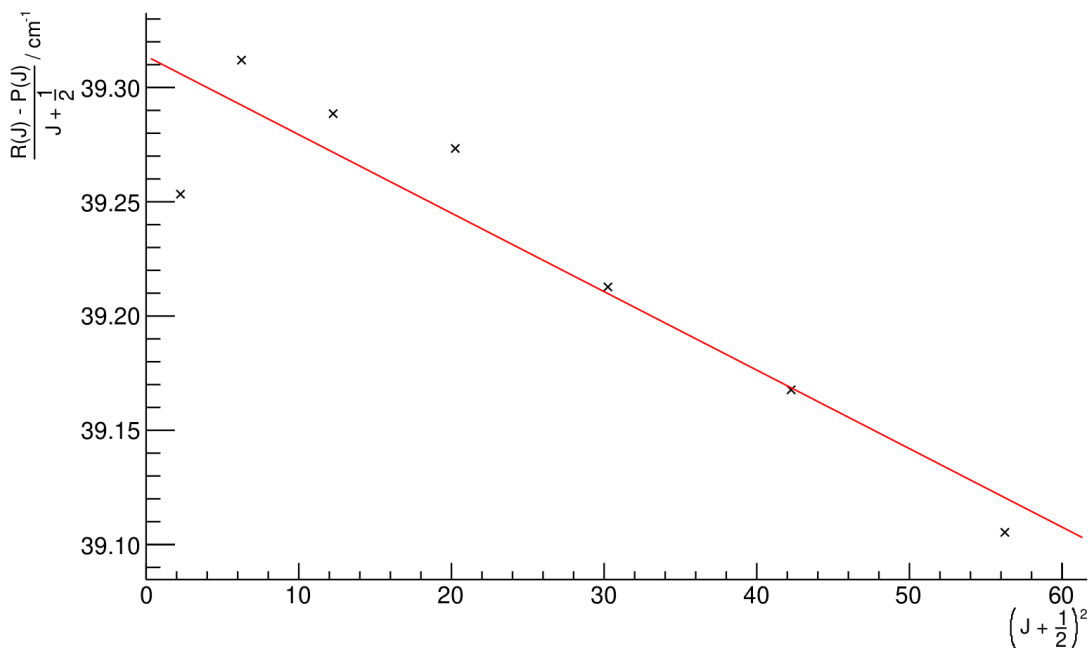

Figure 2: Graph showing the linear regression performed for the upper rotational (R) branch for the overtone transition in $H^{35}Cl$.

The bond lengths in table 3 were determined from the $\tilde{B}_\nu$ values using equation 1.2.5. Furthermore the calculus-based approximation[2] was utilised to propagate the uncertainties in $\tilde{B}_\nu$ for r_ν (α_{r_ν}) as the $\alpha_{\tilde{B}_\nu}$ values are small hence producing equation 1.2.6. The uncertainties in the values of the constants and reduced mass used[3] are insignificant compared to that of $\alpha_{\tilde{B}_\nu}$, and hence they were excluded from the error propagation.

$$r_\nu = \sqrt{\frac{h}{8\pi^2 c\mu \tilde{B}_\nu}} \tag{1.2.5}$$

$$\alpha_{r_\nu} = \frac{1}{2}\sqrt{\frac{h}{8\pi^2 c\mu \tilde{B}_\nu{}^3}}\,\alpha_{\tilde{B}_\nu} \tag{1.2.6}$$

Table 3: Rotational constants and bond lengths.

	ν	$\tilde{B}_\nu$ / cm^{-1}	$\tilde{B}_{\nu_{Lit.}}$ / cm^{-1}	r_ν / pm
	0	10.4408 ± 0.0004	$10.439\,82$	128.823 ± 0.002
H^{35}Cl	1	10.1360 ± 0.0002	$10.132\,64$	130.745 ± 0.001
	2	9.829 ± 0.004	$9.825\,46$	132.77 ± 0.02
	0	10.4248 ± 0.0003		128.385 ± 0.002
H^{37}Cl	1	10.1214 ± 0.0001		130.2953 ± 0.0009
	2	9.86 ± 0.02		132.0 ± 0.1

1.3   Determination of Vibrational Constants

The harmonic constant, $\tilde{\nu}_e$, and the anharmonicity constant, x_e, in table 4 were determined using equations 1.3.1 and 1.3.2. The derivation method of these equations is included in section 3.2 within the supplementary information.

$$\tilde{\nu}_e = R(0) - 3\tilde{B}_1 + \tilde{B}_2 \tag{1.3.1}$$

$$x_e = \frac{1}{2}\frac{\tilde{B}_2 - \tilde{B}_1}{R(0) - 3\tilde{B}_1 + \tilde{B}_2} \tag{1.3.2}$$

The uncertainties in these values was estimated using equations 1.3.3 and 1.3.4 with the uncertainty in $R(0)$ excluded from the propagation as it is negligible compared to that in $\tilde{B}_1$ and $\tilde{B}_2$ since it is determined by reading the absorption wavenumber directly from the spectrum.

$$\alpha_{\tilde{\nu}_e} = \sqrt{\left(3\alpha_{\tilde{B}_1}\right)^2 + \left(\alpha_{\tilde{B}_2}\right)^2} \tag{1.3.3}$$

$$\alpha_{x_e} = x_e \sqrt{\frac{\left(\alpha_{\tilde{B}_1}\right)^2 + \left(\alpha_{\tilde{B}_2}\right)^2}{\left(\tilde{B}_2 - \tilde{B}_1\right)^2} + \left(\frac{\alpha_{\tilde{\nu}_e}}{\tilde{\nu}_e}\right)^2} \tag{1.3.4}$$

Table 4: Vibrational Coefficients.

	H^{35}Cl	H^{37}Cl
$\tilde{\nu}_e$ / cm^{-1}	2885.821 ± 0.004	2883.78 ± 0.02
x_e / 10^{-5}	-5.32 ± 0.06	-4.5 ± 0.3

1.4   Determination of Bond Force Constants

The bond force constants, k, in table 5 were determined using equation 1.4.1 and the error in k, α_k, was determined using equation 1.4.2 (derived using the calculus-based approximation). The errors in μ and the constants were again not considered as they are negligible compared to that of ν_e.

$$k = 4\pi^2 c^2 \mu \tilde{\nu}_e{}^2 \tag{1.4.1}$$

$$\alpha_k = 8\pi^2 c^2 \mu \tilde{\nu}_e \alpha_{\tilde{\nu}_e} = 8\pi^2 c^2 \mu \tilde{\nu}_e \sqrt{\left(3\alpha_{\tilde{B}_1}\right)^2 + \left(\alpha_{\tilde{B}_2}\right)^2} \tag{1.4.2}$$

Table 5: Force Constants.

	$H^{35}Cl$	$H^{37}Cl$
k / $N\,m^{-1}$	477.383 ± 0.001	480.698 ± 0.006

2 Discussion

2.1 Errors and Analysis Method

It is likely that the errors used for the data collected are underestimates since they are derived from linear regressions performed with a limited number of data points (less than 12). Furthermore while the linear regression was (in general) good for the data obtained for fundamental transitions ($\chi^2 = 2 \times 10^{-5}$–$2 \times 10^{-4}$) it was much poorer for data derived from the overtone transition ($\chi^2 = 4 \times 10^{-4}$–$0.2$). This was due to the considerable signal:noise ratio on the spectrum for the overtone transition resulting in the data being significantly effected by random noise (as can be seen in figure 2) and hence the true uncertainty in these values is likely to be even greater.

There is a high signal:noise ratio for the data from the overtone transition compared to that of the fundamental due to the lower overtone transition probability as the transition is forbidden by the $\Delta\nu = \pm 1$ selection rule for a purely harmonic potential and while the oscillator in anharmonic it still has considerable harmonic character. This signal:noise ratio could be reduced by recording additional spectra for just the overtone region (6000–5000 cm^{-1}) with a greater concentration of HCl in the gas cell. The reduced wavenumber range should be used since the increased concentration will also increase the intensity of the fundamental transition peaks and will cause them to be 'cut' hence preventing a distinct wavenumber from being recorded for the fundamental transition absorption peak.

In the data analysis the centrifugal distortion was accounted for since when it was ignored the linear regression produced residuals which were clearly not randomly distributed hence suggesting the presence of a systematic error. When the centrifugal distortion was accounted for the residual plot showed a more random distribution.

2.2 Data

2.2.1 Rotational Constants

The value of $\tilde{B}_0$ could have been obtained by considering either the fundamental or overtone transition. The value tabulated in table 3 was derived from the fundamental transition since less random noise affected the values for the fundamental transition (as discussed in section 2.1, hence using only this transition reduced the random errors in the value determined.

It was expected that the values of $\tilde{B}_\nu$ for $H^{35}Cl$ should be larger than the corresponding values for $H^{37}Cl$ due to the greater reduced mass of the $H^{37}Cl$ isotopologue making the $\tilde{B}_\nu$ value larger by equation 2.2.1.

$$\tilde{B}_\nu = \frac{h}{8\pi^2 c \mu r^2} \tag{2.2.1}$$

The obtained data (presented in table 3) supports this since all values of $\tilde{B}_\nu$ calculated for $H^{35}Cl$ are greater than the corresponding values for $H^{37}Cl$ except for the $\tilde{B}_2$ value where this condition can be satisfied with a probability of 6.06 % (calculated by assuming a normal distribution around the data point

and normalising). As discussed in section 2.1 it is likely the errors used are underestimates hence the agreement of this datum with the expected result is likely to be stronger than this.

The data for $\tilde{B}_\nu$ in table 3 all agree with the literature values, $\tilde{B}_{\nu_{Lit.}}$, within $\pm 0.004\,\mathrm{cm}^{-1}$. While this is one order of magnitude greater than the estimated uncertainties in all values (except for $\tilde{B}_2$) it is likely that the obtained data does agree with these literature values, however (as discussed in section 2.1) the uncertainties stated are underestimates.

In order to obtain better estimates of the uncertainties for the rotational constants additional spectra could be recorded hence allowing a better estimation of the uncertainty in the calculated values based any differences which arise between the data sets collected. This will also help suggest the reproducibility of the collected data.

2.2.2 Bond Lengths

It was also expected that the bond length (r_ν) values for both isotopologues would increase as the vibrational energy level (ν) increased since the anharmonicity of the bond potential results in the mean bond length increasing as the vibrational energy level increases. All of the values of r_ν obtained in table 3 agree with this.

In table 3 it can also be seen that the bond lengths of the $H^{37}Cl$ isotopologue in each vibrational state are greater than for the $H^{35}Cl$ isotopologue. This is the expected result since from the one dimensional time-independent Schrödinger equation (equation 2.2.2) it can be seen that for the same potential function $V(x)$ (assumed since the chemical bonding should identical for both isotopologues) and molecular (stationary) states described by ψ_ν the energy of the state labelled by ν will decrease for an increased reduced mass. Hence from the asymmetry of the anharmonic bond potential the $H^{37}Cl$ isotopologue should have a lower mean bond length in each vibrational state.

$$
\begin{aligned}
E_\nu \psi_\nu &= \hat{H}\psi_\nu \\
&= \left(\frac{\hat{p}^2}{2\mu} + V(x) \right) \psi_\nu
\end{aligned}
\tag{2.2.2}
$$

2.2.3 Bond Force Constants

It was expected that the bond force constants, k, displayed in table 5 should be equal for both isotopologues as it was assumed that k depends only on the chemical bonding and hence should be the same for both isotopologues.

Despite this the force constants differ by $3.315\,\mathrm{N\,m}^{-1}$ while both values have very small uncertainties of the order of 1×10^{-3}. It is unlikely that an underestimation of the uncertainties in the $\tilde{B}_0$ and $\tilde{B}_1$ values can explain this difference since if the uncertainties in the $\tilde{B}_0$ and $\tilde{B}_1$ values for both isotopologues are increased by a factor of ten (this would hence give good agreement between the $\tilde{B}_0$ and $\tilde{B}_1$ values for $H^{35}Cl$ and the literature values) then when this is propagated the uncertainty in the bond constants also increases by slightly more than a factor of ten. This results in a difference between the bond constants of over 500 standard deviations.

It is considered unlikely that a systematic error could result in the difference between the calculated bond force constants since both were obtained from taking differences between values on the spectrum (which should remove systematic errors) and both values were obtained from the same spectrum thus removing the influence of any calibration errors.

It is possible that the mass of a molecule affects the bond force constant in an indirect way as concluded by Biernacki and Clerjaud for the SiH_4 and SiD_4 isotopologues.[4] In order to confirm this with more confidence more spectra should be recorded of the overtone and fundamental transitions (as discussed in 2.1 and 2.2.1). In addition to this further spectra could be obtained for deuterated hydrogen chloride gas, DCl,

since this will increase the reduced mass by almost a factor of two, hence should result in an even larger difference in the bond force constants.

References

(1) K. Huber and G. Herzberg, *Constants of Diatomic Molecules*, ed. P. Linstrom and W. Mallard, (data prepared by J.W. Gallagher and R.D. Johnson, III) in NIST Chemistry WebBook, NIST Standard Reference Database Number 69, `https://doi.org/10.18434/T4D303` (visited on 04/12/2018).

(2) I. G. Hughes and T. P. A. Hase, *Measurements and their Uncertainties*, Oxford University Press, Oxford, 2010.

(3) *CRC Handbook of Chemistry and Physics*, ed. W. M. Haynes, CRC Press, Boca Raton, 97th edn., 2016.

(4) S. W. Biernacki and B. Clerjaud, *Physical Review B*, 2001, **63**, 075201-1 –075201-6.

3 Supplementary Information

3.1 Centrifugal Distortion Coefficients

The values of the centrifugal distortion coefficients, $\tilde{D}_\nu$, were determined from the gradient found by completing linear regressions.

Table 6: Centrifugal distortion coefficients.

	ν	$\tilde{D}_\nu$ / 10^{-4} cm^{-1}
	0	5.25 ± 0.04 and 5.4 ± 0.3
^{35}Cl	1	5.11 ± 0.02
	2	4.3 ± 0.8
	0	5.20 ± 0.03 and 9 ± 2
^{37}Cl	1	5.13 ± 0.01
	2	11 ± 4

3.2 Derivation of Vibrational Constant Equations

The energies associated with the discrete vibrational energy levels in a molecule are given by equation 3.2.1 which can be found through the application of perturbation theory on the harmonic potential with the perturbation of the potential including terms a of higher order than two from the Taylor expansion of the potential energy.

$$\tilde{E}_\nu = \tilde{\nu}_e \left(\nu + \frac{1}{2} \right) - \tilde{\nu}_e x_e \left(\nu + \frac{1}{2} \right)^2 \tag{3.2.1}$$

From equation 3.2.1 we can obtain the energy related to the pure vibrational transition $\tilde{E}(\nu_f \leftarrow 0)$ (the $\nu = 0$ to $\nu = \nu_f$ transition) as equation 3.2.2.

$$\begin{aligned} \tilde{E}(\nu_f \leftarrow 0) &= \tilde{E}_{\nu_f} - \tilde{E}_0 \\ &= \tilde{\nu}_e \left(\nu_f + \frac{1}{2} - \frac{1}{2} \right) - \tilde{\nu}_e x_e \left(\frac{1}{4} - \left(\nu_f + \frac{1}{2} \right)^2 \right) \\ &= \tilde{\nu}_e \left(\nu_f - \left(\nu_f^2 + \nu_f \right) x_e \right) \end{aligned} \tag{3.2.2}$$

The energy related to the R branch transitions can be determined to yield equation 3.2.3 where J is the rotational state adopted in the lower vibrational state ($\nu = 0$).

$$R(J) = \Delta \tilde{E}(\nu_f \leftarrow 0) + (\tilde{B_{\nu_f}} + \tilde{B}_0)(J+1) + (\tilde{B_{\nu_f}} - \tilde{B}_0)(J+1)^2 \tag{3.2.3}$$

Setting $J = 0$ hence gives equation 3.2.4.

$$R(J) - 2\tilde{B}_{\nu_f} = \Delta\tilde{E}(\nu_f \leftarrow 0) \tag{3.2.4}$$

Substituting equation 3.2.2 into equation 3.2.4 yields equation 3.2.5.

$$R(0) - 2\tilde{B}_{\nu_f} = \tilde{\nu}_e \left(\nu_f - \left(\nu_f^2 + \nu_f \right) x_e \right) \tag{3.2.5}$$

Now from equation 3.2.5 a system of linear equations can be obtained by setting $\nu_f = 1$ and $\nu_f = 2$ (equations 3.2.6 and 3.2.7).

$$R(0) - 2\tilde{B}_1 = \tilde{\nu}_e \left(1 - 2x_e \right) \tag{3.2.6}$$

$$R(0) - 2\tilde{B}_2 = \tilde{\nu}_e \left(1 - 6x_e \right) \tag{3.2.7}$$

Solving equations 3.2.6 and 3.2.7 for $\tilde{\nu}_e$ and x_e then gives equations 1.3.1 and 1.3.2.